

DETECTION OF INTRA-DAY VARIABILITY TIMESCALES OF FOUR HIGH ENERGY PEAKED BLAZARS WITH XMM-NEWTON

HARITMA GAUR¹, ALOK C. GUPTA¹, PAWEŁ LACHOWICZ^{2, 3}, PAUL J. WIITA^{4, 5}

Accepted for publication in ApJ 2010 May 23

ABSTRACT

We selected a sample of 24 XMM-Newton light curves (LCs) of four high energy peaked blazars, PKS 0548–322, ON 231, 1ES 1426+428 and PKS 2155–304. These data comprise continuous light curves of 7.67h to 18.97h in length. We searched for possible quasi-periodic oscillations (QPO) and intra-day variability (IDV) timescales in the LCs of these blazars. We found a likely QPO in one LC of PKS 2155–304 which was reported elsewhere (Lachowicz et al. 2009). In the remaining 23 LCs we found hints of possible weak QPOs in one LC of each of ON 231 and PKS 2155–304, but neither is statistically significant. We found IDV timescales that ranged from 15.7 ks to 46.8 ks in 8 LCs. In 13 LCs any variability timescales were longer than the length of the data. Assuming the possible weak QPO periods in the blazars PKS 2155–304 and ON 231 are real and are associated with the innermost portions of their accretion disk, we can estimate that their central black hole masses exceed $1.2 \times 10^7 M_{\odot}$. Emission models for radio-loud active galactic nuclei (AGN) that could explain our results are briefly discussed.

Subject headings: galaxies: active – BL Lacertae objects: general – BL Lacertae objects: individual (PKS 0548–322; ON 231; 1ES 1426+428; PKS 2155–304)

1. INTRODUCTION

Blazars, including BL Lacertae objects (BL Lacs) and flat spectrum radio quasars (FSRQs), are extragalactic radio sources with relativistic jets aligned nearly ($\lesssim 10^\circ$) with the line of sight (e.g., Urry & Padovani 1995). Blazar emission extends across the entire electromagnetic (EM) spectrum, is predominantly nonthermal, and shows significant polarization in the radio and visible bands where it can be measured. Blazars show detectable flux variations on diverse timescales ranging from a few minutes through days and months to decades through all EM bands. Blazar variability timescales have often been somewhat arbitrarily divided into three classes: timescales from minutes to less than a day are called intra-day variability (IDV); those from several days to a few months are known as short timescale variability (STV); while long term variability (LTV) covers changes from several months to many years (e.g., Gupta et al. 2004).

Short and intra-day X-ray variability has been investigated in various classes of AGNs (e.g., Edelson & Nandra 1999; Uttley et al. 2002; Markowitz et al. 2003; Vaughan et al. 2003b; McHardy et al. 2004, 2005; Espaillat et al. 2008; Lachowicz et al. 2009; and references therein). The great majority of these studies have been done for the brighter sources, which are typically nearby Seyfert

galaxies, and were reviewed recently by Uttley (2007). There were claims of the detection of QPOs in a few AGNs on the short and IDV timescales in early X-ray observations (Fiore et al. 1989; Papadakis & Lawrence 1993; Iwasawa et al. 1998). But all of these claimed QPO detections were later found to be not statistically significant (Tagliaferri et al. 1996; Benlloch et al. 2001; Vaughan 2005; Vaughan & Uttley 2006). There have, however, been few stronger claims of QPO detection recently in X-ray data of various classes of AGNs. The first significant detection of a short X-ray QPO of ~ 1 hour timescale has been reported for RE J1034+396, which is a narrow line Seyfert 1 galaxy (Gierliński et al. 2008). Espaillat et al. (2008) have reported an X-ray QPO on the timescale of 3.3 ks in 3C 273, a FSRQ. Very recently, Lachowicz et al. (2009) have reported a detection of a X-ray QPO in the BL Lac PKS 2155–304 on a timescale of ~ 4.6 hours. All three of these QPO detections on IDV timescales were based on observations made with XMM-Newton. By using All Sky Monitor data from the Rossi X-ray Timing Explorer, Rani et al. (2009) have reported a probable QPO from the BL Lac AO 0235+164 on a STV timescale of ~ 18 days. Such QPOs may shed new light on the physical processes at the source and associated X-ray emission and so the search for their presence in the light curves (LCs) of AGN is important.

The full spectral energy distributions (SEDs) of blazars have double humped structures with each large spectral peak having comparable total powers. In these double humped SEDs, the first (lower energy) component of the SED is quite clearly dominated by synchrotron radiation from the relativistic jet and the second component is probably due to Inverse-Compton (IC) radiation. On the basis of their SEDs, blazars can be classified into two subclasses known as LBLs (Low-Energy Peaked Blazars) and HBLs (High Energy Peaked Blazars), though those with intermediate peaks are certainly found (Nieppola

haritma@aries.res.in, acgupta30@gmail.com, pawel@ieee.org, wiita@chandra.stonybrook.edu

¹ Aryabhata Research Institute of Observational Sciences (ARIES), Manora Peak, Nainital - 263129, India

² Nicolaus Copernicus Astronomical Center, Polish Academy of Sciences, ul. Bartycka 18, 00-716 Warszawa, Poland

³ Center for Wavelets, Approximations and Information Processing, Temasek Laboratories, National University of Singapore, 5A Engineering Dr 1, # 09-02 Singapore 117411

⁴ Department of Physics and Astronomy, Georgia State University, P.O. Box 4106, Atlanta, GA 30302-4106

⁵ Department of Physics, The College of New Jersey, P.O. Box 7718, Ewing, NJ 08628

et al. 2006). In LBLs, the synchrotron component peaks at near-IR, optical or near-UV frequencies and the high energy component usually peaks at GeV energies. In HBLs, the synchrotron component peaks somewhere in the X-ray band and the high energy component is seen to peak (or is extrapolated to do so) at TeV energies.

Here, we study four HBLs which are designated as TeV blazars because of their significant detections in that extreme energy band. Just six years ago only six TeV blazars were known (see Krawczynski et al. 2004 for a summary of their properties). Thanks to the development of new TeV facilities such as HESS (High Energy Stereoscopic System; Hofmann et al. 2003; Funk et al. 2004. Aharonian et al. 2006), MAGIC (Major Atmospheric Gamma-ray Imaging Cerenkov; Baixeras et al. 2004; Cortina et al. 2005; Albert et al. 2006a) and VERITAS (Very Energetic Radiation Imaging Telescope Array System; Holder et al. 2006; Maier 2007, Maier et al. 2008) there has been a complete revolution in TeV gamma-ray astronomy. These groups have detected about a dozen new TeV emitting blazars (HBLs) (Albert et al. 2006b, 2007, 2008, 2009; Acciari et al. 2008, 2009a, 2009b; Aharonian et al. 2007, 2008a, 2008b, 2008c, 2008d, 2009a, 2009b, 2009c, and references therein). The enlarged sample of TeV blazars will be very useful for our understanding of the emission mechanism of these extreme blazars through the study of their variability properties across the range of EM bands. Here, we report our search for X-ray variability on IDV timescales in four HBLs from the XMM-Newton satellite public archive. We plan to perform extensive variability studies of HBLs in other EM bands using ground based observations.

The motivation of this work is to examine the nature of IDV in a sample of four high energy peaked blazars, namely, PKS 0548–322, ON 231, 1ES 1426+428 and PKS 2155–304, in which synchrotron emission from the jets dominates up through the X-ray component. We will use IDV data to search for QPOs (quasi-periodic oscillations) and variability timescales in the light curves (LCs) of these HBLs, recalling that the shortest timescales can give upper limits to the sizes of the emitting regions. When a blazar is in a low flux state it is possible that an accretion disk related component of the X-ray emission is dominant and then any IDV timescale could give an estimate of the mass of the black hole presumed to reside at the center of the galaxy (e.g., Gupta et al. 2008, 2009). This possibility arises from the fact that some blazars show evidence of the “big blue bump” that is almost certainly indicative of accretion disk emission (e.g., Raiteri et al. 2007) while in their low states, when the jets are weak or even absent. Under these circumstances the X-ray corona expected above such disks and observed in radio-quiet AGN should be visible. A break in the power spectral density (PSD) plot from intra-day LCs can also yield the black hole mass of the blazar (e.g., Uttley 2007). XMM-Newton IDV LCs also may possibly be used to make independent estimations of the Doppler factors of the blazars (Fan, Xie & Bacon 1999).

The paper is structured as follows. In Section 2, we give brief descriptions of the data selection criterion and the data reduction method. In Section 3, we discuss the techniques we used to search for variability properties and provide the results in Section 4. Our discussion is in Section 5 and the conclusions are given in Section 6.

2. XMM-NEWTON DATA SELECTION AND PROCESSING

2.1. Data Selection Criteria

We selected our four target high energy peaked blazars, namely: PKS 0548–322, ON 231, 1ES 1426+428, and PKS 2155–304 because they were observed by the European Photon Imaging Camera (EPIC) on board the XMM-Newton satellite (Jansen et al. 2001). Instead of analyzing data from previous or other current X-ray missions, we used data from XMM-Newton/EPIC due to its excellent detector sensitivity, a wide field of view that allows for good background subtraction, and the ability to track the source continuously for many hours.

The EPIC is composed of three co-aligned X-ray telescopes (Jansen et al. 2001) which simultaneously observe a source by accumulating photons in three CCD-based instruments: the twins MOS 1 and MOS 2 and the pn (Turner et al. 2001; Strüder et al. 2001). The EPIC instrument provides imaging and spectroscopy in the energy range from 0.15 to 15 keV with a good angular resolution (PSF = 6 arcsec FWHM) and a moderate spectral resolution ($E/\Delta E \approx 20 - 50$).

From the XMM-Newton Science Archive⁶ we downloaded 24 data sets of these four blazars which satisfy the key selection criteria that the observation exceeds 7 hours and the source was bright enough to give adequate counts in short time bins. These criteria allow us to possibly obtain reasonable indications of intra-day timescales as well as QPOs with periods up to at least one hour. These constraints yielded 1 data set for PKS 0548–322, 1 for ON 231, 7 observations of 1ES 1416+428 and 15 stars at PKS 2155–304. These 24 observations took place between 30 May 2000 and 12 May 2008 and lasted between 7.67 hours and 18.97 hours. In this paper we omit further consideration of the observations made on 1 May 2006 of PKS 2155–304 which showed a significant QPO at ~ 4.6 hours and was reported in Lachowicz et al. (2009). The observing log for the remaining 23 X-ray observations is given in Table 1, the first four columns of which contain the blazar name, date of the observation, name of the principal investigator, and length of the data for that observation.

2.2. Data reduction

To perform the data reduction we used pipeline products and applied the XMM-Newton Science Analysis System (SAS) version 8.0.0 for the LC extraction. The first step in this reduction is to check for strong proton flares in the 10–12 keV range. We confined our analysis to EPIC/pn data as only they were free of soft-proton flaring events and pile-up effects. We had to restrict our analysis to the 0.3 – 10 keV energy range, as data below 0.3 keV are mostly unrelated to bona fide X-rays, and data above 10 keV are usually dominated by background. Next, the data are extracted using a circle of 45 arcsec radius centered on the source. Background photons are read out from the same size area located about 180 arcsec off the source on the same chipset. Then raw light curves for both the target and background areas are produced. As the final product of data reduction, we obtained source LCs for the 0.3–10 keV band (cor-

⁶ <http://xmm.esac.esa.int/xsa/>

Table 1. Observation log of XMM-Newton data for high energy peaked blazars

Source	$\alpha_{2000.0}$	$\delta_{2000.0}$	z	Date of Observation dd.mm.yyyy	PI	GTI ^a (ks)	Timescale(ks)	σ_{frac}	μ (cts s ⁻¹)
PKS0548–322	05h 50m 41.0s	–32° 16′ 11″.0	0.069	11.10.2002	Xavier Barcons	45.5	Not Found	2.65	13.82±0.03
ON 231	12h 21m 31.7s	+28° 13′ 58″.5	0.102	26.06.2002	Keith Mason	27.6	Weak QPO? ^b	31.58	1.89±0.06
1ES1426+428	14h 28m 32.7s	+42° 40′ 21″.0	0.129	16.06.2001	Bert Brinkman	62.0	46.8	3.49	11.95±0.04
				04.08.2004	Fred Jansen	61.9	Not Found	2.69	14.43±0.04
				06.08.2004	Fred Jansen	68.3	Not Found	2.71	14.39±0.04
				24.01.2005	Fred Jansen	29.8	Not Found	2.51	18.01±0.06
				19.06.2005	Fred Jansen	37.9	Not Found	2.33	26.57±0.05
				25.06.2005	Fred Jansen	33.9	Not Found	2.13	20.77±0.05
				04.08.2005	Fred Jansen	39.9	Not Found	2.27	20.22±0.05
PKS2155–304	21h 58m 52.1s	–30° 13′ 31″.1	0.116	30.05.2000	Arvind Parmar	37.9	24.2	2.89	54.76±0.05
				31.05.2000	Arvind Parmar	59.2	41.2	3.27	54.86±0.04
				19.11.2000	Laura Maraschi	57.2	Not Found	9.76	49.51±0.04
				20.11.2000	Laura Maraschi	58.1	16.0	4.04	40.37±0.04
				30.11.2001	Arvind Parmar	44.5	Not Found	7.60	80.88±0.05
				24.05.2002	Fred Jansen	31.7	24.2	6.54	39.51±0.06
				24.05.2002	Fred Jansen	31.6	Weak QPO? ^b	2.90	28.17±0.06
				24.05.2002	Fred Jansen	29.8	Not Found	20.74	38.30±0.06
				29.11.2002	Arvind Parmar	56.7	26.8	10.94	21.29±0.04
				23.11.2004	Fred Jansen	39.8	15.7	4.08	28.78±0.05
				30.11.2005	Fred Jansen	49.8	Not Found	9.34	54.52±0.04
				07.11.2006	Arvind Parmar	28.8	Not Found	3.94	29.68±0.06
				22.04.2007	Arvind Parmar	48.0	41.4	9.93	50.69±0.05
				12.05.2008	Arvind Parmar	60.6	Not Found	7.32	62.26±0.04

^a GTI (Good Time Interval) is determined by screening data for soft-proton flare using the selection criteria ($\#$ XMMEA_EP and $10000 < \text{PI} < 12000$) and (PATTERN = 0) for the EPIC/pn camera, and thus requires the total count rate to be below 0.4 cts/s within the 10–12 keV energy band.

^b See text for details

rected for background flux and given in unit of counts s⁻¹), sampled evenly with a fixed bin size of $\Delta t = 0.1$ ks.

In column 5 of Table 1 we report the variability timescale, if present. The sixth column contains the fractional rms variability, defined as $\sigma_{frac} = (\sigma^2/\mu^2)^{1/2}$, where σ^2 is the mean variance (counts² s⁻²) (Uttley & McHardy 2001) and μ is the mean flux (0.3 – 10 keV, counts s⁻¹), which is given in the last column. The left columns of panels in Figures 1–4 display these LCs.

3. ANALYSIS TECHNIQUES

3.1. Structure Function Analysis

We used the first order structure function (SF) for our first time series analysis. The SF is a powerful tool to quantitatively determine periodicities and time scales in time series data (e.g., Rutman 1978; Simonetti et al. 1985; Paltani et al. 1997). It provides information on the time structure of a data train and it is able to discern the range of the characteristic time scales that contribute to the fluctuations. It is less affected by any data gaps in the LCs and is free of the constant offset in the time series. The first order SF for a data set a , having uniformly sampled points, is defined as

$$D_a(k) = \frac{1}{N'_a(k)} \sum_{i=1}^n \omega(i)\omega(i+k)[a(i+k) - a(i)]^2, \quad (1)$$

where k is the time lag, $N'_a(k) = \sum \omega(i)\omega(i+k)$, and the weighting factor $\omega(i)$ is 1 if a measurement exists for the i^{th} interval and 0, otherwise.

The square of the uncertainty in the estimated SF is

$$\sigma^2(k) = \frac{8\sigma_{df}^2}{N'(k)} D_a(k), \quad (2)$$

where σ_{df}^2 is the measured noise variance. Here the lags

were examined in units of 0.1 ks, the fixed bin size of our uniformly sampled data.

The behavior of the first order SF indicates the presence (or not) of a timescale in the LC as follows: a) if the source's first order SF rises and does not display any plateau, it implies that any time scale of its variability is longer than the length of the observation; b) if there are one or more plateaus, each one may indicate a time scale of variability; c) if that plateau is followed by a dip in the SF, the temporal lag corresponding to the minimum of that dip suggests a possible periodic cycle. If a LC contains cycles of period P , $SF(dt)$ will rise to a maximum at $dt = P/2$ and then fall to a minimum at $dt = P$ (Smith et al. 1993). When dt is extended to values that are nearly multiples of P , $SF(dt)$ itself goes through a series of cycles. Any possible periods extracted from a SF analysis are obtained by averaging the trough-to-trough times. The plots of these SF analyses are presented in the center columns of Figs. 1–4 and the strongest timescales estimated from them are given in the fifth column of Table 1.

3.2. Power Spectral Density

A classical tool in the search for the nature of temporal variations, including any periodic and quasi-periodic variability in a LC, employs calculations of the Fourier power spectral density (PSD). In general, it is expected that a power-law model, $P(f) \propto f^\alpha$ where α denotes the spectral slope, is a good representation of the red-noise variability ($\alpha < 0$) that characterizes most blazars (e.g. Kataoka et al. 2001; Zhang et al. 2002). In general, one assumes that any significant positive deviation above that red-noise model (i.e., $\gtrsim 3\sigma$) can stand for a clear indication of a quasi-periodic oscillation (QPO) being present in the X-ray emission (see Vaughan et al. 2003a; Vaughan & Uttley 2006, and references therein). Because of a lack of high quality data and the appar-

Table 2. The best power-law fits to power spectra^a

Source	Date of Observation dd.mm.yyyy	α	$\log(N)$	χ^2/ν	ν^c
PKS0548–322	11.10.2002	-2.11 ± 0.88	-9.72	0.31	4
ON 231	26.06.2002	-2.11 ± 0.32	-5.96	36.98	22
1ES1426+428	16.06.2001	-2.44 ± 0.86	-10.31	1.19	4
	04.08.2004	-2.27 ± 0.86	-10.32	0.13	4
	06.08.2004	-0.97 ± 0.59	-4.38	0.52	8
	24.01.2005	-1.00 ± 0.36	-4.19	0.15	18
	19.06.2005	-2.33 ± 0.76	-9.79	0.61	5
	25.06.2005	-1.91 ± 1.61	-8.53	0.52	1
	04.08.2005	-2.46 ± 1.23	-10.91	0.20	2
PKS2155–304	30.05.2000	-3.52 ± 0.76	-14.68	0.62	5
	31.05.2000	-2.15 ± 0.33	-8.62	0.55	21
	19.11.2000	-1.91 ± 0.19	-6.53	1.21	55
	20.11.2000	-2.01 ± 0.29	-7.71	5.34	27
	30.11.2001	-1.76 ± 0.22	-6.09	1.00	42
	24.05.2002	-1.88 ± 0.27	-6.84	3.13	29
	24.05.2002	-1.68 ± 0.38	-6.32	0.87	17
	24.05.2002	-1.98 ± 0.19	-6.02	5.00	57
	29.11.2002	-2.65 ± 0.46	-10.03	15.63	12
	23.11.2004	-1.88 ± 0.37	-6.88	2.25	17
	30.11.2005	-2.29 ± 0.24	-8.02	5.68	37
	07.11.2006	-1.91 ± 0.33	-6.84	1.47	21
	22.04.2007	-2.19 ± 0.24	-7.79	1.60	36
	12.05.2008	-2.04 ± 0.21	-7.40	0.71	46

^a The power-law model is assumed to be $P(f) \propto f^\alpha$ for $\alpha < 0$ ^b The errors are 1σ ^c Degrees of freedom (d.o.f.)

ently low duty cycles of their QPOs, the PSDs of powerful AGN were not found to display convincing QPO features in studies made over the last three decades. The very recent discoveries of QPOs in a narrow line Seyfert 1 galaxy (Gierliński et al. 2008) a FSRQ (Espaillat et al. 2008) and a BL Lac (Lachowicz et al. 2009) show that they are sometimes present and definitely worth searching for.

Here, we employ a standard approach (e.g., van der Klis 1989; Vaughan et al. 2003a) in which we use the normalization of PSD after Miyamoto et al. (1992) that provides the PSD in units of $(\text{rms}/\text{mean})^2/\text{Hz}$. We compute all our Fourier power spectra using the DFT subroutine in MATLAB[®], and fit the resultant red-noise part of the PSD, where applicable, using a code based on Vaughan’s (2005) recipe. We model each red-noise component as a single power-law function,

$$P(f) = N f^\alpha, \quad (3)$$

in the low-frequency portion of the power spectrum, i.e., where the red-noise variability at the longest timescales starts to dominate over the white-noise level present at the highest frequencies.

The results are presented in Figs. 1–4, where the histogram, solid line, dotted line and horizontal dashed line denote the PSD, red-noise component of the PSD, 99.73% (3σ) confidence level for the red-noise model, and the expected Poisson noise level, respectively. Table 2 lists the best values for the two parameters of the fitted red-noise model (a slope α and normalization N) and the goodness-of-fit measure, χ^2/ν , for the number of degrees-of-freedom, $\nu = m - 2$, where m equals the number of frequency bins involved in the fit.

4. RESULTS

4.1. PKS 0548–322

PKS 0548–322 is a nearby BL Lac object and is hosted in a giant elliptical galaxy (Falomo Pesce & Treves 1995; Wurtz et al. 1996) which is the dominant member of a rich cluster of galaxies. Imaging and spectroscopic observations of the field around the source show that it is at a redshift of $z = 0.069$ (Falomo et al. 1995). The synchrotron power peaks in the X-ray band, and for this reason it is classified as an HBL source (Padovani & Giommi 1995).

In the span of 30 nights of observations, (Cruz-Gonzalez & Huchra 1984) noticed a typical ~ 0.02 mag (2%) day^{-1} optical variability in the source. The source was monitored by Xie et al. (1996) in the V-band for IDV and they once reported a rise of 0.58 magnitudes over an interval of 5 minutes. Optical IDV of this source was also studied for a few nights in 1995–1996 by Bai et al. (1998).

PKS 0548–322 is a relatively strong and rapidly variable source in the X-ray energy bands (Blustin et al. 2004). The possibility of deviation from a single power law in the X-ray spectrum has been present since early observations of this source. It was observed by EXOSAT during 1983 to 1986 (Barr et al. 1988; Garilli & Maccagni 1990) and its SED peaked in the 2.5–5 keV energy range. GINGA observations in February, 1991 (Tashiro et al. 1995) of the 2–30 keV energy range showed a flatter spectrum, with the synchrotron peak of the SED moved to energies higher than 30 keV. This blazar was observed by BeppoSAX in 1999 during February through April (Costamante et al. 2001). PKS 0548–322 was observed by the Swift satellite (Gehrels et al. 2004) during April through June of 2005 and the spectral analysis of its X-ray telescope (XRT) data was reported by Burrows et al. (2005) and that from the Ultraviolet/Optical telescope (UVOT) was discussed by Roming et al. (2005). These data confirmed that the X-ray spectrum of this HBL shows a well established curvature (Perri et al. 2007) for which evidence had been found by Costamante et al. (2001).

Stecker et al. (1996) predicted VHE gamma-ray fluxes from this object. The CANGAROO (Collaboration of Australia and Nippon for a Gamma Ray Observatory in the Outback) group have reported limits to the VHE gamma-ray emission above ~ 1.5 TeV for the source (Roberts et al. 1998). VHE gamma-ray observations were also made with the Mark 6 telescope (Armstrong et al. 1999) and 3σ limits to the VHE gamma-ray flux of $2.4 \times 10^{-11} \text{ cm}^{-2} \text{ sec}^{-1}$ above 300 GeV for the source was reported by Chadwick et al. (2000). The source was, however, detected at the threshold energy of 190 GeV by HESS with an integrated flux of $6.65 \times 10^{-12} \text{ cm}^{-2} \text{ s}^{-1}$ (Aharonian et al. 2005a). This source has not yet been detected by the FERMI satellite (Abdo et al. 2010).

This blazar PKS 0548–322 was continuously monitored by XMM-Newton for 45.5 ks on October 11, 2002 and the rather flat LC we extracted from this data is given in the first panel in Fig. 1. The SF we produced from this observation is plotted as the middle panel in the first row of Fig. 1. This SF plot shows a continuous rising trend as the temporal lag increases. Therefore any variability timescale that might have been present at that time is larger than the length of the data set.

The power spectrum analysis of our single data set for

PKS 0548–322 revealed the variability pattern to be in a good agreement with a model dominated by a broad-band white noise process, i.e., $P(f) \propto f^0$. However, at the longest accessible timescales (or lowest frequencies) there is good evidence for a contribution from red-noise variability (right column of the first row in Fig. 1 and Table 2).

4.2. ON 231

ON 231 was previously known as the “variable star” W Comae (and is still also called by that name). In 1971, because of its odd properties, particularly a strong optical variability and an apparently line-less continuum, it was suggested that it was an extragalactic source and was assigned to the then rather new class of BL Lac objects (Biraud 1971; Browne 1971). The later detection of weak emission lines in its spectrum during a time when the synchrotron optical emission was less dominant made it possible to determine its redshift, $z = 0.102$ (Weistrop et al. 1985).

The historical B passband LC of the source (during 1935–1997) was plotted by Tosti et al. (1998). It has shown optical flux variations on diverse timescales ranging from a few hours to several years (Xie et al. 1992; Smith & Nair 1995). In 1995, ON 231 started a phase of strong brightness and activity that culminated in an outburst in April–May 1998, when it reached its brightest magnitude at $R = 12.2$ (Massaro et al. 1999) comparable to that measured at the beginning of the past century when it was discovered as a variable star (Wolf 1916). After the optical outburst, ON 231 showed a slow decline in its mean luminosity (Tosti et al. 2002). Photometric observations on January 2007 in the Johnson R passband found the source to be in a low state (Gupta et al. 2008) comparable to the faintest state ever noted by Tosti et al. (1998).

BeppoSAX observed the source in May 1998 with good sensitivity and spectral resolution, following the exceptional outburst that occurred in April–May of that year. The sensitivity of the WFC (Wide Field Camera) on BeppoSAX depends on the pointing direction, but for an AGN at high-galactic latitude it is possible to determine the spectrum up to 200 keV for sources with fluxes down to about 1mCrab (Boella et al. 1997). An X-ray spectrum was measured from 0.1–100 keV and a smaller variability amplitude between 0.4–10 keV was detected (Tagliaferri et al. 2000). Massaro et al. (2008) studied the spectral energy distribution of the source using Swift UV data, along with soft X-ray data from three Swift/XRT pointings.

ON 231 was discovered as a gamma-ray source (von Montigny et al. 1995) and was detected by EGRET in the 100 MeV to 10 GeV band (Hartman et al. 1999). This source exhibited the hardest spectrum among the EGRET AGN detections (Sreekumar et al. 1996). A strong gamma-ray outburst in W Com which lasted for 4 days was observed in March 2008; VHE gamma-ray emission was detected by VERITAS with a statistical significance of 4.9σ for the data set of January–April 2008 (Acciari et al. 2008).

The XMM-Newton satellite continuously monitored ON 231 for 27.6 ks on 26 June 2002 and its LC and SF are plotted in the second row of Fig. 1. The LC shows considerable variability, with the flux changing by

a factor of about three during this, the shortest of all the observations we considered. The SF plot starts with a continuous rising trend to a maximum, followed by a dip; the SF then rises and dips two more times. The peaks in the SF are at 10.4, 15.7 and 22.6 ks, while the minima following them are at 12.0, 19.9 and 27.1 ks, respectively. The last of these dips is too close to the total length of the observation to be meaningful. The nominal variability time scales are taken as the differences between maxima and previous minima, or 10.4 ks, 3.7 ks ($= 15.7 - 12.0$) and 2.7 ks ($= 22.6 - 19.9$). The first dip might provide evidence for a periodicity at 12.0 ks, but as the subsequent dips are not at multiples of this value, no claim for periodicity can be made from this LC using the SF.

Our Fourier analysis of the LC of ON 231 is given in the last column of the second row of Fig. 1. It reveals that the overall profile of the broad-band variability of ON 231 can be described by a single power-law with a slope $\alpha = -2.11 \pm 0.32$, extending down to timescales of $1/f \simeq 1000$ s. (This best fit is achieved, however, at a poor reduced $\chi^2/\nu = 36.98$ for $\nu = 22$ degrees of freedom.) This, and other (usually much better) best fits to the PSD slopes for the other blazars, along with the number of degrees-of-freedom used to estimate the red-noise portion of the PSD, are given in Table 2. Interestingly, this PSD also showed a statistically insignificant ($< 2\sigma$) peak located at $\sim 1.7 \times 10^{-4}$ Hz, suggesting a possible very weak QPO with period close to ~ 5.9 ks. However, as this possible timescale differs from any of those hinted at by the SF for ON 231, we certainly cannot claim that any significant quasi-periodicity was present in this blazar at the time of this observation.

4.3. 1ES 1426+428

The blazar 1ES 1426+428 now thought to be at $z = 0.129$ was discovered in the medium X-ray band (2–6 keV) with the Large Area Sky Survey experiment (LASS) on HEAO-1 (Wood et al. 1984). It was classified as a BL Lac object on the basis of its featureless optical spectrum. Observations made with the MDM 2.4 m Hiltner telescope constrained its redshift to $z \geq 0.106$ (Finke et al. 2008) and its host galaxy was resolved by Urry et al. (2000). Remillard et al. (1989) reported its radio flux is 33.7 mJy at 1.4 GHz and they also presented its optical spectrum.

In X-rays, 1ES 1426+428 is bright, with a 2–6 keV luminosity $\sim 10^{44}$ ergs sec $^{-1}$ (assuming isotropic emission), which is typical of HEAO-1 (High Energy Astronomical Observatory) BL Lac objects (Schwartz et al. 1989). X-ray observations of the source were carried out by Costamante et al. (2001) with BeppoSAX and the X-ray spectrum was found to extend up to 100 keV. An X-ray absorption feature was detected in 1ES 1426+428 by Sambruna et al. (1997) which led to the exploration of the gaseous environment of BL Lac objects. Falcone et al. (2004) observed 1ES 1426+428 with the Rossi X-Ray Timing Explorer (RXTE) and found that the peak energy in the SED was sometimes in the excess of 100 keV and at other times in the 2.4–24 keV region.

This source has been observed in the TeV gamma-ray band by CAT (Cerenkov Array at Themis) and HEGRA (High Energy Gamma Ray Astronomy) (Djannati-Atai

et al. 2002; Petry et al. 2000; Aharonian et al. 2002, 2003; Horan et al. 2002). Observations made with the MAGIC telescope gave an upper limit of γ -ray flux at 200 GeV is 5.5×10^{-12} ergs cm $^{-2}$ s $^{-1}$ (Albert et al. 2008). The intrinsic spectrum of 1ES 1426+428 was inferred by Costamante et al. (2003) using a model spectrum of the extragalactic background light (EBL) given by Primack et al. (2001). Aharonian et al. (2003) obtained a rising intrinsic source spectrum in the TeV regime, using the same EBL spectra that Costamante et al. (2003) and Malkan & Stecker (2001) adopted.

The blazar 1ES 1426+428 was continuously monitored by XMM-Newton for 62.0 ks on 16 June 2001 and its LC and SF on that day are plotted in the third row of Fig. 1. The SF plot shows a continuous rising trend followed by a dip which indicates variability time scale of 46.8 ks. However, this was the only possible time scale seen for this blazar, which was also continuously monitored for 61.9, 68.3, 29.8, 37.9, 33.9, 39.9 ks on 4 August 2004, 6 August 2004, 24 January 2005, 19 June 2005, 25 June 2005, and 4 August 2005, respectively. All these LCs and their SFs are plotted in Figs. 1 and 2. The SF plots of all these LCs have continuous rising trends, so any variability timescales associated with these LCs are longer than the lengths of the observations.

We have found that the Fourier power spectra for four of the seven observations of 1ES 1426+428 blazar do not display any significant red-noise components, with only possible indications of red-noise at the lowest few bins in temporal frequency. Power-law red-noise is best seen on 16 June 2001 ($\alpha = -2.44 \pm 0.86$; $\chi^2/\nu = 1.19$ for $\nu = 4$). Red noise is weakly detectable on 6 August 2004 and 24 January 2005, respectively (see the right columns of Figs. 1 and 2 and Table 2). Neither the SF nor PSD techniques indicate any hints of QPOs in this blazar, and only one indication of a timescale of variability was detected via the SF analysis at 46.8 ks, which was longer than four of the seven observations.

4.4. *PKS 2155–304*

PKS 2155–304 was first identified as a BL Lac by Schwartz et al. (1979) and Hewitt & Burbidge (1980), and is the brightest BL Lac object from the UV to TeV energies in the southern hemisphere. It had already been observed in the radio as part of the Parkes survey (Shimmins & Bolton 1974). Since the 1970’s, it has been observed on diverse timescales by many space and ground based telescopes in all EM bands (e.g., Carini & Miller 1992; Urry et al. 1993; Brinkmann et al. 1994; Marshall et al. 2001; Aharonian et al. 2005b; Dominici, Abraham & Galo 2006; Dolcini et al. 2007; Piner, Pant & Edwards 2008; Sakamoto et al. 2008; and references therein). A redshift of 0.117 ± 0.002 was given by Bowyer et al. (1984) but careful spectroscopy of galaxies in the field of PKS 2155–304, by Falomo et al. (1993) demonstrated that the redshift of the source is 0.116 ± 0.002 . Simultaneous observations of PKS 2155–304 in the optical and near-infrared bands showed significant variability on a wide range of timescales (e.g., Domini, Abraham & Galo 2006; Osterman et al. 2007; Dolcini et al. 2007). PKS 2155–304 has shown a linear optical polarization of 3–7% with a polarization position angle varying between 70° and 120° (Tommasi et al. 2000).

Schwartz et al. (1979) reported the first X-ray observa-

tions of PKS 2155–304 using HEAO-1. It has been suggested that the synchrotron emission of PKS 2155–304 tends to peak in the UV-EUV rather than in the X-rays (Zhang 2008). Simultaneous multi-wavelength observations of this blazar from X-ray (using XMM-Newton) and optical bands are presented by Zhang et al. (2006a). Using XMM-Newton observations from EPIC pn data, hardness ratio variations and temporal cross-correlations between bands were computed and discussed by Zhang et al. (2006b) who found the variations between bands were more strongly correlated during flares.

PKS 2155–304 was classified as a TeV blazar by the detection of VHE gamma-rays by the Durham MK 6 telescopes (Chadwick et al. 1999). It was confirmed as a high energy gamma-ray emitter by HESS at a 45σ significance level (Aharonian et al. 2005b) and it is so bright that IDV is also detectable in the this VHE band.

Observations in the UV by the International Ultraviolet Explorer of PKS 2155–304 seemed to show a short-lived quasi-period of ~ 0.7 day, but only a few cycles were present, so it was not a firm detection (Urry et al. 1993). Recently, we have shown nominally very strong evidence for a ~ 4.6 hour QPO in this source in XMM-Newton observations made on 1 May 2006; but again, as only ~ 4 cycles of this fluctuation were seen during about 18 hours of the observation, the QPO indication is not iron-clad (Lachowicz et al. 2009).

The blazar PKS 2155–304 was continuously monitored by XMM-Newton for 57.2, 44.5, 29.8, 49.8, 28.8, and 60.6 ks on 19 November 2000, 30 November 2001, 24 May 2002, 30 November 2005, 07 November 2006, and 12 May 2008, respectively. There was no evidence for timescales on those days. These LCs and their SFs are plotted in Figs. 2–4. As the SF plots of all these light curves show continuous rising trends, any variability timescale for these LCs are longer than the lengths of their data trains.

This source also was continuously monitored for 37.9 ks on 30 May 2000, 59.2 ks on 31 May 2000, 58.1 ks on 20 November 2000, 31.7 ks on 24 May 2002, 56.7 ks on 29 November 2002, 39.8 ks on 23 November 2004, and 48.0 ks on 22 April 2007 and during these observations indications of timescales were found. These LCs and their SFs are also plotted in Figs. 1 and 2. Each of these SF plots show a continuous rising trend followed by a dip. These dips indicate possible variability time scales of 24.2 ks, 41.2 ks, 16.0 ks, 24.2 ks, 26.8 ks, 15.7 ks and 41.4 ks, respectively.

During the second observation made of PKS 2155–304 on 24 May 2002, we detected four dips in the SF that might indicate a weak QPO signal (see the fourth row of Fig. 3). For this data set the SF remains quite flat for the first ~ 5.3 ks, indicative of white noise domination at short lags or high frequencies (e.g., Paltani et al. 1997). The SF then rises to a peak at 8.8 ks, indicating a timescale of 3.5 ks, where we follow Paltani et al. (1997) and subtract the 5.3 ks before the SF started its rise. The first dip in the SF is at ~ 12.2 ks, providing a hint of a period at 6.9 ks ($= 12.2 - 5.3$ ks). The timescales for the subsequent rises to peaks following minima are 2.6 ks, 2.5 ks and 3.0 ks, while the three subsequent dips yield “periods” of 4.8 ks, 4.6 ks and 7.0 ks, as measured from the previous dips. Although these times between dips are clearly not the same, and therefore do not give

a clear indication of a single period, if one averages the four “periods” obtained from the dip intervals then one obtains a broad “quasi-period” of 5.5 ± 1.3 ks, although two separate timescales of ~ 4.7 ks and ~ 7.0 ks are an alternative possibility. For the same observation, the PSD analysis provides us with a possible indication of a weak ($< 2\sigma$) peak centered around $\sim 1.7 \times 10^{-4}$ Hz (see Fig. 3). That would also suggest a QPO period of ~ 5.9 ks, which is, coincidentally, a value close to that we noted for a possible QPO in ON 231.

A quantitative analysis of all 14 PSDs of PKS 2155–304 allowed us to find its broad-band X-ray variability to be very well described for most observations by a single power-law component denoting red-noise at lower frequencies with white noise present at high frequencies. As seen from Figs. 2–4, for about half of these data sets this power-law extended over the great majority of the frequency band we could measure, while for the other half the white noise dominated a significant portion of it. The results of the best fit slope values over the red-noise dominated portions are given in Table 2 and range from $-3.5 \leq \alpha \leq -1.7$. In the data discussed here the only hint of quasi-periodic variability detected in the X-ray PSDs of this was the observation on 24 May 2002 mentioned in the previous paragraph.

5. DISCUSSION

The generally accepted models for the strong variability in blazars on LTV timescales (months to decades) involve shocks propagating down relativistic jets pointing close to the direction from which we observe them (e.g. Scheuer & Readhead 1979; Marsher & Gear 1985; Wagner & Witzel 1995). These shocks moving through jets almost certainly dominate the fluctuations in BL Lacs at essentially all phases and in FSRQs when they are in high flux states. The shorter STV and IDV variations can be most simply explained in terms of irregularities in the jet flows and any possible periodic variability has been suggested to arise from shocks passing through nearly helical structures in a jet (e.g., Camenzind & Krockenberger 1992), by jets whose orientation with respect to us changes (e.g., Gopal-Krishna & Wiita 1992) or by turbulence behind a shock (Marscher, Gear & Travis 1992). Instabilities on or above accretion disks also should play a role in luminosity fluctuations for FSRQs, particularly in lower luminosity states, and they presumably dominate in non-blazar AGNs such as Seyfert galaxies (e.g., Abramowicz et al. 1991; Mangalam & Wiita 1993; Wagner & Witzel 1995).

The X-ray emission we are concerned with here, however, is unlikely to arise from the disk itself and is usually attributed to coronal flares above the disk in non-blazar AGN (e.g. di Matteo 1998) and to jet emission in blazars (e.g. Böttcher 2007). Some recent work has argued that the nuclear emission in low luminosity radio-loud AGNs indicates that the accretion disk is radiatively inefficient (e.g., Balmaverde et al. 2006; Balmaverde & Capetti 2006). If this is correct, the emission in even the low luminosity radio-loud AGNs that are likely the parent population of BL Lacs is dominated by non-thermal emission from the base of the jet.

Now X-ray flares not far above the inner part of a disk might well have fluctuations closely related to the disk’s orbital period. As most of the quasi-thermal radiation

from an accretion disk emerges from its innermost portion, the relevant orbital period and/or size of the emitting region is most likely to be at, or at least close to, that of the last stable circular orbit around the central supermassive black hole (SMBH) that is allowed by general relativity. If the variability does arise in this way, then one can compute a rough estimate of the mass, M , of the SMBH which is proportional to the period (e.g. Gupta et al. 2009):

$$M/M_{\odot} = 3.23 \times 10^4 P(s) [(r^{3/2} + (a/M))^{-1} (1+z)^{-1}] \quad (4)$$

where $P(s)$ is a period of some fluctuations (in seconds), r is the radius of the emitting region within the disk in units of GM/c^2 and a/M is the dimensionless BH angular momentum parameter. For the possible periods of ~ 5.9 ks seen in one PKS 2155–304 data set and in the single ON 231 data set this corresponds to $\sim 1.2 \times 10^7 M_{\odot}$ for a non-rotating SMBH (with $r = 6$, the last stable circular orbit for a disk around a Schwarzschild BH with $a/M = 0$) and $\sim 7.4 \times 10^7 M_{\odot}$ for a rapidly rotating SMBH (with $r = 1.2$, the last stable circular orbit for a co-rotating disk around an physically maximally spinning BH with $a/M = 0.998$; e.g., Thorne 1974). We again wish to stress that neither of those QPO signals are statistically significant, as their peaks in the PSD plots do not reach the usually adopted 3σ threshold (Vaughan 2005) for significance of a QPO with respect to the underlying red-noise source variability defined by a single power-law model.

Still, because most blazar emission is expected to arise from jets that are launched from the immediate vicinity of the SMBH rather than the disk or its corona, (e.g. Marscher et al. 2008), the observed timescale, P_{obs} , of any fluctuation is likely to be reduced with respect to the rest-frame timescale, P_{em} , by the Doppler factor, δ , as well as increased by a factor of $(1+z)$. As usual, the Doppler factor, δ , is defined in terms of the velocity of the jet (and/or the shock propagating down the jet), V , and the angle between the jet and the observer’s line-of-sight, θ , as $\delta = [\Gamma(1 - \beta \cos\theta)]^{-1}$; we have adopted the standard notation, $\beta = V/c$ and $\Gamma = (1 - \beta^2)^{-1/2}$. Hence, $P_{obs} = P_{em}/\delta$. From very high energy gamma-ray observations of PKS 0548–322, $18 < \delta < 25$ was estimated (Superina et al. 2008). Radio observations indicate that ON 231 has $1.2 < \delta < 5.2$ (Wu et al. 2007; Hovatta et al. 2009). From INTEGRAL observations at 150 keV, $\delta \simeq 27.3$ was proposed for 1ES 1426+428 (Wolter et al. 2008). Finally, from high to very high energy gamma-ray observations $\delta > 30$ was obtained for PKS 2155–304 (Urry et al. 1997; Ghisellini & Tavecchio 2008). The fluctuations could be induced by the disk rotation and then advected into the jet where they could become responsible for variations in the jet density, velocity or magnetic field (e.g., Wiita 2006). In that case the amplitude of the variation would be greatly enhanced by Doppler boosting (roughly as δ^3) while time-compressed by δ^{-1} (e.g., Gopal-Krishna et al. 2003). This boosting could possibly make even weak disk variations detectable once amplified by the jets. In that case the SMBH mass estimates would rise by a factor of δ . Taking the average of the δ values quoted for ON 231 (3.2), the nominal SMBH mass estimates would rise to $3.8 \times 10^7 M_{\odot}$ for the non-rotating case and $2.4 \times 10^8 M_{\odot}$ for the rapidly

spinning case. If $\delta = 30$ for PKS 2155–304 then the estimates for the SMBH mass would be between $3.6 \times 10^8 M_\odot$ and $2.2 \times 10^9 M_\odot$, with the bounds corresponding to non- and rapidly- rotating situations. Such higher values are in better agreement with most estimates for the masses of SMBHs, ($> 2 \times 10^8 M_\odot$) in powerful radio loud AGN (e.g., Dunlop et al. 2003), but those masses may not be directly applicable to HBLs. Because the galaxies surrounding the AGN in most HBLs, including ON 231 and PKS 2155–304, are barely detected and the optical spectra of the AGN are essentially featureless, no other techniques usually can be applied to provide alternative SMBH mass estimates for these HBLs. However, to give an indicative mass for an HBL, we note that stellar velocity dispersions have been measured for a number of low- z BL Lacs, including 0548–322, for which a SMBH mass of $\simeq 1.4 \times 10^8 M_\odot$ has been estimated (Barth, Ho & Sargent 2003).

6. CONCLUSIONS

From our structure function analysis of high quality archival X-ray light curves of four HBLs taken by the XMM-Newton EPIC/pn detector between May 2000 to May 2008, we found only one apparently significant possible detection of a QPO which we have presented in detail elsewhere (Lachowicz et al. 2009). This was discovered using the SF method for PKS 2155–304 at a timescale of ≈ 16.7 ks. This estimated QPO was confirmed by three other essentially independent methods, viz, a periodogram analysis, a wavelet analysis and a careful power spectrum density analysis along the lines of Vaughan (2005) that gave a probability of > 0.9973 that a real signal had been seen; however, the short length of the data train compared to the nominal period still means that we cannot make a firm claim for the presence of a QPO (Lachowicz et al. 2009).

Here we have presented the remaining 23 LCs, none of

which showed any significant detections of QPOs. One out of these 14 observations of PKS 2155–304 showed four dips in the SF, which might conceivably indicate a broad QPO around 5.8 ks but a PSD analysis of the same observation gave a only a very weak hint of one at 5.9 ks. The one data set available for ON 231 showed three dips in the SF that did not provide any significant period while the PSD analysis gave a weak signal corresponding to a possible QPO around 5.9 ks. We stress that no significant signal was seen in the PSD plots for any of these 23 observations. We did find evidence for time scales ranging from 15.7 ks to 46.8 ks in eight additional LCs using SF analyses; one of these was for 1ES 1426+428 and the other seven for PKS 2155–304. Combining our new results for PKS 2155–304 along with those of Urry et al. (1993) and Lachowicz et al. (2009) it is clear that this blazar is well worth continued observations to search for timescales and possible QPOs. For the remaining 13 LCs, any variability timescale that may be present seems to be longer than the length of the X-ray data sets, which ranged from 29 to 68 ks. For none of these data sets were the individual measurements long enough to clearly see a break in the PSD at low frequencies that could also provide a handle on SMBH masses (e.g., Marshall, Ryle & Miller 2007). Although multi-wavelength campaigns are necessary to properly understand the emission regions and processes in blazars, lengthy and frequent monitoring in single bands, such as has been done with XMM-Newton, can provide interesting constraints.

We thank the anonymous referee for many suggestions that significantly improved the presentation of this paper. This research is based on observations obtained with XMM-Newton, an ESA science mission with instruments and contributions directly funded by ESA member states and NASA.

REFERENCES

- Abdo, A. A., & for the Fermi-LAT Collaboration 2010, arXiv:1002.0150
- Abramowicz, M. A., Bao, G., Lanza, A., & Zhang, X.-H. 1991, A&A, 245, 454
- Acciari, V. A., et al. 2008, ApJ, 684, L73
- Acciari, V., et al. 2009a, ApJ, 690, L126
- Acciari, V. A., et al. 2009b, ApJ, 703, L6
- Aharonian, F., et al. 2002, A&A, 384, L23
- Aharonian, F., et al. 2003, A&A, 403, 523
- Aharonian, F., et al. 2005a, A&A, 441, 465
- Aharonian, F., et al. 2005b, A&A, 442, 895
- Aharonian, F., et al. 2006, A&A, 457, 899
- Aharonian, F., et al. 2007, A&A, 473, L25
- Aharonian, F., et al. 2008a, A&A, 490, 685
- Aharonian, F., et al. 2008b, A&A, 484, 435
- Aharonian, F., et al. 2008c, A&A, 481, L103
- Aharonian, F., et al. 2008d, A&A, 481, 401
- Aharonian, F., et al. 2009a, A&A, 499, 723
- Aharonian, F., et al. 2009b, ApJ, 695, L40
- Aharonian, F., et al. 2009c, ApJ, 692, 1500
- Albert, J., et al. 2006a, ApJ, 638, L101
- Albert, J., et al. 2006b, ApJ, 642, L119
- Albert, J., et al. 2007, ApJ, 667, L21
- Albert, J., et al. 2008, ApJ, 681, 944
- Albert, J., et al. 2009, A&A, 493, 467
- Armstrong, P., et al. 1999, Experimental Astronomy, 9, 51
- Bai, J. M., Xie, G. Z., Li, K. H., Zhang, X., & Liu, W. W. 1998, A&AS, 132, 83
- Baixaeras, C., et al. 2004, Nuclear Instruments and Methods in Physics Research A, 518, 188
- Balmaverde, B., & Capetti, A. 2006, A&A, 447, 97
- Balmaverde, B., Capetti, A., & Grandi, P. 2006, A&A, 451, 35
- Barr, P., Giommi, P., & Maccagni, D. 1988, ApJ, 324, L11
- Barth, A.J., Ho, L.C., & Sargent, W.L.W. 2003, ApJ, 583, 134
- Benlloch, S., Wilms, J., Edelson, R., Yaqoob, T., & Staubert, R. 2001, ApJ, 562, L121
- Biraud, F. 1971, Nature, 232, 178
- Blustin, A. J., Page, M. J., & Branduardi-Raymont, G. 2004, A&A, 417, 61
- Boella, G., Butler, R. C., Perola, G. C., Piro, L., Scarsi, L., & Bleeker, J. A. M. 1997, A&AS, 122, 299
- Böttcher, M. 2007, Ap&SS, 309, 95
- Bowyer, S., Brodie, J., Clarke, J. T., & Henry, J. P. 1984, ApJ, 278, L103
- Brinkmann, W., et al. 1994, A&A, 288, 433
- Browne, I. W. A. 1971, Nature, 231, 515
- Burrows, D. N., et al. 2005, Space Science Reviews, 120, 165
- Camenzind, M. & Krockenberger, M. 1992, A&A, 255, 59
- Carini, M. T., & Miller, H. R. 1992, ApJ, 385, 146
- Chadwick, P. M., et al. 1999, ApJ, 513, 161
- Chadwick, P. M., et al. 2000, A&A, 364, 450
- Costamante, L., Aharonian, F., Ghisellini, G., & Horns, D. 2003, New Astronomy Review, 47, 677
- Cortina, J., et al. 2005, International Cosmic Ray Conference, 5, 359
- Costamante, L., et al. 2001, A&A, 371, 512
- Cruz-Gonzalez, I., & Huchra, J. P. 1984, AJ, 89, 441
- di Matteo, T. 1998, MNRAS, 299, L15
- Djannati-Atai, A., et al. 2002, A&A, 391, L25
- Dolcini, A., et al. 2007, A&A, 469, 503
- Dominici, T. P., Abraham, Z., & Galo, A. L. 2006, A&A, 460, 665
- Dunlop, J. S., McLure, R. J., Kukula, M. J., Baum, S. A., O’Dea, C. P., & Hughes, D. H. 2003, MNRAS, 340, 1095
- Edelson, R., & Nandra, K. 1999, ApJ, 514, 682
- Espallat, C., Bregman, J., Hughes, P., & Lloyd-Davies, E. 2008, ApJ, 679, 182

- Falcone, A. D., Cui, W., & Finley, J. P. 2004, *ApJ*, 601, 165
- Falomo, R., Pesce, J. E., & Treves, A. 1993, *ApJ*, 411, L63
- Falomo, R., Pesce, J. E., & Treves, A. 1995, *ApJ*, 438, L9
- Fan, J. H., Xie, G. Z., & Bacon, R. 1999, *A&AS*, 136, 13
- Fiore, F., Massaro, E., Perola, G. C., & Piro, L. 1989, *ApJ*, 347, 171
- Finke, J. D., Shields, J. C., Böttcher, M., & Basu, S. 2008, *A&A*, 477, 513
- Funk, S., et al. 2004, *Astroparticle Physics*, 22, 285
- Garilli, B., & Maccagni, D. 1990, *A&A*, 229, 88
- Gehrels, N., et al. 2004, *ApJ*, 611, 1005
- Ghisellini, G., & Tavecchio, F. 2008, *MNRAS*, 386, L28
- Gierliński, M., Middleton, M., Ward, M., & Done, C. 2008, *Nature*, 455, 369
- Gopal-Krishna, Stalin, C. S., Sagar, R., & Wiita, P. J. 2003, *ApJ*, 586, L25
- Gopal-Krishna & Wiita, P. J. 1992, *A&A*, 259, 109
- Gupta, A. C., Banerjee, D. P. K., Ashok, N. M., & Joshi, U. C. 2004, *A&A*, 422, 505
- Gupta, A. C., Deng, W. G., Joshi, U. C., Bai, J. M., & Lee, M. G. 2008, *New Astronomy*, 13, 375
- Gupta, A. C., Srivastava, A. K., & Wiita, P. J. 2009, *ApJ*, 690, 216
- Hartman, R. C., et al. 1999, *ApJS*, 123, 79
- Hewitt, A., & Burbidge, G. 1980, *ApJS*, 43, 57
- Hofmann, W., & H. E. S. S. Collaboration 2003, *International Cosmic Ray Conference*, 5, 2811
- Holder, J., et al. 2006, *Astroparticle Physics*, 25, 391
- Horan, D., et al. 2002, *ApJ*, 571, 753
- Hovatta, T., Valtaoja, E., Tornikoski, M., Lähteenmäki, A. 2009, *A&A*, 494, 527
- Iwasawa, K., Fabian, A. C., Brandt, W. N., Kunieda, H., Misaki, K., Terashima, Y., & Reynolds, C. S. 1998, *MNRAS*, 295, L20
- Jansen, F., et al. 2001, *A&A*, 365, L1
- Kataoka, J., Takahashi, T., Edwards, P. G., Wagner, S. J., Inoue, S., & Takahara, F. 2001, in *High Energy Gamma-Ray Astronomy*, American Institute of Physics Conference Series, 558, 660
- Krawczynski, H., et al. 2004, *ApJ*, 601, 151
- Lachowicz, P., Gupta, A. C., Gaur, H., & Wiita, P. J. 2009, *A&A*, 506, L17
- Malkan, M. A., & Stecker, F. W. 2001, *ApJ*, 555, 641
- Maier, G. 2007, arXiv:0709.3661
- Maier, G., Acciari, V. A., Amini, R., et al. 2008, in *Proc. 30th International Cosmic Ray Conference*, Vol. 3, ed. R. Caballero et al. (Mexico City: UNAM), p. 1457
- Mangalam, A. V., & Wiita, P. J., 1993, *ApJ*, 406, 420
- Markowitz, A., et al. 2003, *ApJ*, 593, 96
- Marshall, H. L., Urry, C. M., Sambruna, R. M., & Pesce, J. E. 2001, *ApJ*, 549, 938
- Marshall, K., Ryle, W. T., & Miller, H. R. 2007, *ApJ*, 677, 880.
- Marscher, A. P., & Gear, W. K. 1985, *ApJ*, 298, 114
- Marscher, A. P., Gear, W. K., & Travis, J. P. 1992, *Variability of Blazars*, ed. E. Valtaoja & M. Valtonen (Cambridge: Cambridge Univ. Press), p. 85
- Marscher, A. P., et al. 2008, *Nature*, 452, 966
- Massaro, E., et al. 1999, *A&A*, 342, L49
- Massaro, F., Tramacere, A., Cavaliere, A., Perri, M., & Giommi, P. 2008, *A&A*, 478, 395
- McHardy, I. M., Gunn, K. F., Uttley, P., & Goad, M. R. 2005, *MNRAS*, 359, 1469
- McHardy, I. M., Papadakis, I. E., Uttley, P., Page, M. J., & Mason, K. O. 2004, *MNRAS*, 348, 783
- Miyamoto S., Kitamoto S., Iga S., Negoro H., Terada K., 1992, *ApJ*, 391, L21
- Nieppola, E., Tornikoski, M., & Valtaoja, E. 2006, *A&A*, 445, 441
- Osterman, M. A., Miller, H. R., Marshall, K., Ryle, W. T., Aller, H., Aller, M., & McFarland, J. P. 2007, *ApJ*, 671, 97
- Padovani, P., & Giommi, P. 1995, *ApJ*, 444, 567
- Paltani, S., Courvoisier, T. J.-L., Blecha, A., & Bratschi, P. 1997, *A&A*, 327, 539
- Papadakis, I. E., & Lawrence, A. 1993, *Nature*, 361, 233
- Perri, M., et al. 2007, *A&A*, 462, 889
- Petry, D., et al. 2000, *ApJ*, 536, 742
- Piner, B. G., Pant, N., & Edwards, P. G. 2008, *ApJ*, 678, 64
- Primack, J. R., Somerville, R. S., Bullock, J. S., & Devriendt, J. E. G. 2001, *American Institute of Physics Conference Series*, 558, 463
- Raiteri, C. M., et al. 2007, *A&A*, 473, 819
- Rani, B., Wiita, P. J., & Gupta, A. C. 2009, *ApJ*, 696, 2170
- Remillard, R. A., Tuohy, I. R., Brissenden, R. J. V., Buckley, D. A. H., Schwartz, D. A., Feigelson, E. D., & Tapia, S. 1989, *ApJ*, 345, 140
- Roberts, M. D., et al. 1998, *A&A*, 337, 25
- Roming, P. W. A., et al. 2005, *Space Science Reviews*, 120, 95
- Rutman, J. 1978, *IEEE Proceedings*, 66, 1048
- Sakamoto, Y., et al. 2008, *ApJ*, 676, 113
- Sambruna, R. M., George, I. M., Madejski, G., Urry, C. M., Turner, T. J., Weaver, K. A., Maraschi, L., & Treves, A. 1997, *ApJ*, 483, 774
- Scheuer, P. A. G., & Readhead, A. C. S. 1979, *Nature*, 277, 182
- Schwartz, D. A., Brissenden, R. J. V., Tuohy, T. R., Feigelson, E. D., Hertz, P. L., & Remillard, R. A. 1989, *BL Lac Objects*, 334, 209
- Schwartz, D. A., Griffiths, R. E., Schwarz, J., Doxsey, R. E., & Johnston, M. D. 1979, *ApJ*, 229, L53
- Shimmins, A. J., & Bolton, J. G. 1974, *Australian Journal of Physics Astrophysical Supplement*, 32, 1
- Simonetti, J. H., Cordes, J. M., & Heeschen, D. S. 1985, *ApJ*, 296, 46
- Smith, A. G., Nair, A. D., Leacock, R. J., & Clements, S. D. 1993, *AJ*, 105, 437
- Smith, A. G., & Nair, A. D. 1995, *PASP*, 107, 863
- Sreekumar, P., et al. 1996, *ApJ*, 464, 628
- Stecker, F. W., de Jager, O. C., & Salamon, M. H. 1996, *ApJ*, 473, L75
- Strüder, L., et al. 2001, *A&A*, 365, L18
- Superina, G., Benbow, W., Boutelier, T., & et al. 2008, *International Cosmic Ray Conference*, 30, 913
- Tagliaferri, G., Bao, G., Israel, G. L., Stella, L., & Treves, A. 1996, *ApJ*, 465, 181
- Tagliaferri, G., et al. 2000, *A&A*, 354, 431
- Tashiro, M., Makishima, K., Ohashi, T., Inada-Koide, M., Yamashita, A., Mihara, T., & Kohmura, Y. 1995, *PASJ*, 47, 131
- Thorne, K. S. 1974, *ApJ*, 191, 507
- Tommasi, L., Díaz, R. J., Pian, E., Mast, D., Palazzi, E., Poretti, E., Scaltriti, F., & Treves, A. 2000, *Boletín de la Asociación Argentina de Astronomía La Plata Argentina*, 44, 91
- Tosti, G., et al. 1998, *A&AS*, 130, 109
- Tosti, G., et al. 2002, *A&A*, 395, 11
- Turner, M. J. L., et al. 2001, *A&A*, 365, L27
- Urry, C. M., & Padovani, P. 1995, *PASP*, 107, 803
- Urry, C. M., et al. 1993, *ApJ*, 411, 614
- Urry, C. M., et al. 1997, *ApJ*, 486, 799
- Urry, C. M., Scarpa, R., O'Dowd, M., Falomo, R., Pesce, J. E., & Treves, A. 2000, *ApJ*, 532, 816
- Uttley, P., & McHardy, I. M. 2001, *MNRAS*, 323, L26
- Uttley, P., McHardy, I. M., & Papadakis, I. E. 2002, *MNRAS*, 332, 231
- Uttley, P. 2007, in *The Central Engine of Active Galactic Nuclei*, ASP Conference Ser., Vol. 373, Eds. L.C. Ho and J.-M. Wang (San Francisco: ASP), p. 149
- van der Klis, M. 1989, *ARA&A*, 27, 517
- Vaughan, S., Edelson, R., Warwick, R. S., & Uttley, P. 2003a, *MNRAS*, 345, 1271
- Vaughan, S., Fabian, A. C., & Nandra, K. 2003b, *MNRAS*, 339, 1237
- Vaughan, S. 2005, *A&A*, 431, 391
- Vaughan, S., & Uttley, P. 2006, *Advances in Space Research*, 38, 1405
- von Montigny, C., et al. 1995, *ApJ*, 440, 525
- Wagner, S. J., & Witzel, A. 1995, *ARAA*, 33, 163
- Weistrop, D., Shaffer, D. B., Hintzen, P., & Romanishin, W. 1985, *ApJ*, 292, 614
- Wiita, P. J. 2006, in *Blazar Variability Workshop II: Entering the GLAST Era*, ASP Conference Series, Vol. 350, Eds., H. R. Miller, K. Marshall, J. R. Webb, and M. F. Aller (San Francisco: ASP), p. 183
- Wolf, M. 1916, *Astronomische Nachrichten*, 202, 415
- Wolter, A., Beckmann, V., Ghisellini, G., Tavecchio, F., & Maraschi, L. 2008, in *Extragalactic Jets: Theory and Observation from Radio to Gamma Ray*, ASP Conf Ser. 386, ed. T. A. Rector & D. S. De Young (San Francisco: ASP), p. 302
- Wood, K. S., et al. 1984, *ApJS*, 56, 507
- Wu, Z., Jiang, D. R., Gu, M., & Liu, Y. 2007, *A&A*, 466, 63
- Wurtz, R., Stocke, J. T., & Yee, H. K. C. 1996, *ApJS*, 103, 109
- Xie, G. Z., Li, K. H., Liu, F. K., Lu, R. W., Wu, J. X., Fan, J. H., Zhu, Y. Y., & Cheng, F. Z. 1992, *ApJS*, 80, 683
- Xie, G. Z., Zhang, Y. H., Li, K. H., Liu, F. K., Wang, J. C., & Wang, X. M. 1996, *AJ*, 111, 1065
- Zhang, Y. H., et al. 2002, *ApJ*, 572, 762
- Zhang, Y. H., Bai, J. M., Zhang, S. N., Treves, A., Maraschi, L., & Celotti, A. 2006a, *ApJ*, 651, 782
- Zhang, Y. H., Treves, A., Maraschi, L., Bai, J. M., & Liu, F. K. 2006b, *ApJ*, 637, 699
- Zhang, Y. H. 2008, *ApJ*, 682, 789

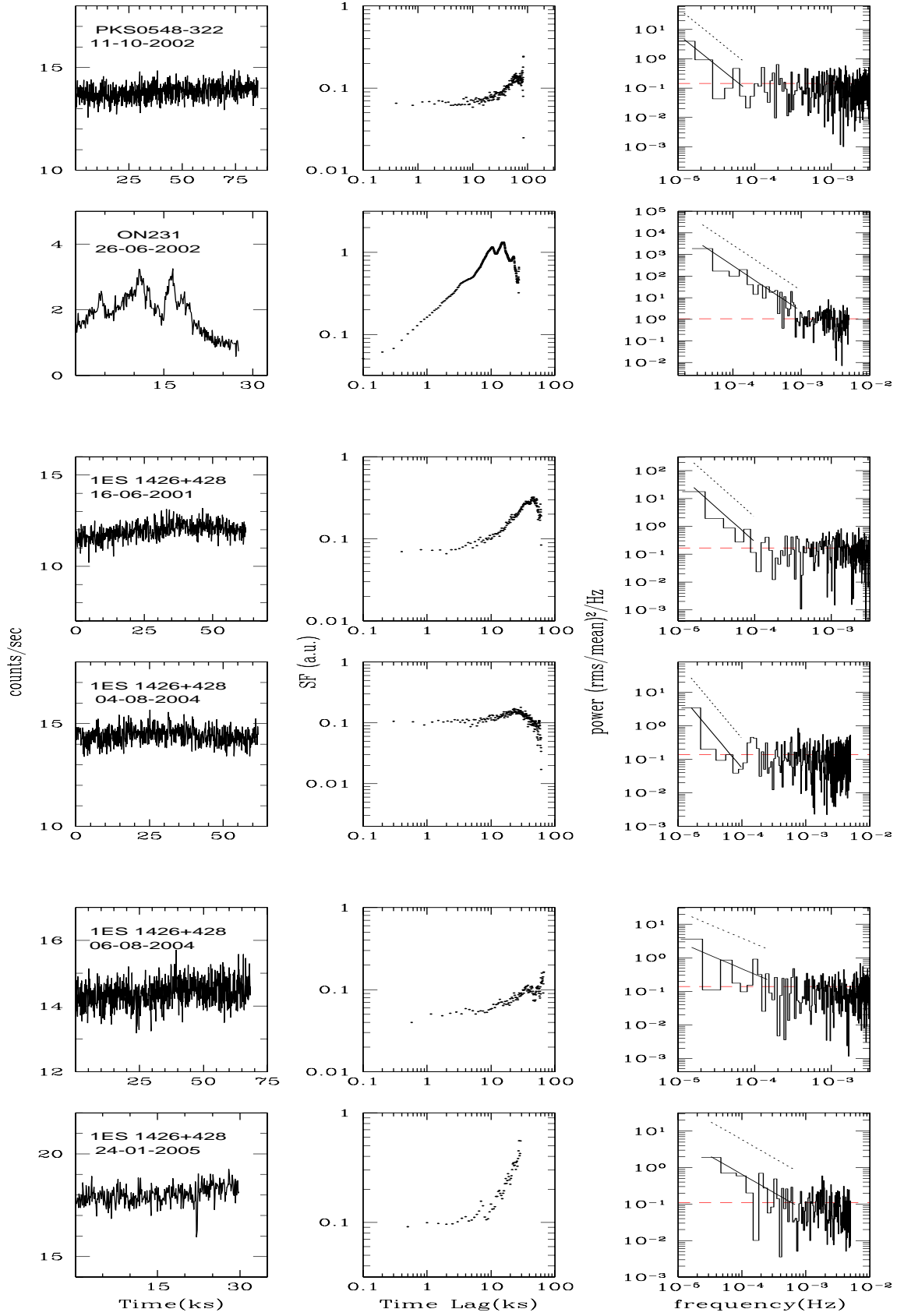


FIG. 1.— Light curves (left panels), structure functions (middle panels) and power spectral densities (right panels) of PKS0548–322, ON 231, and 1ES 1426+428. The source and dates of each observation are given in the light curve panels.

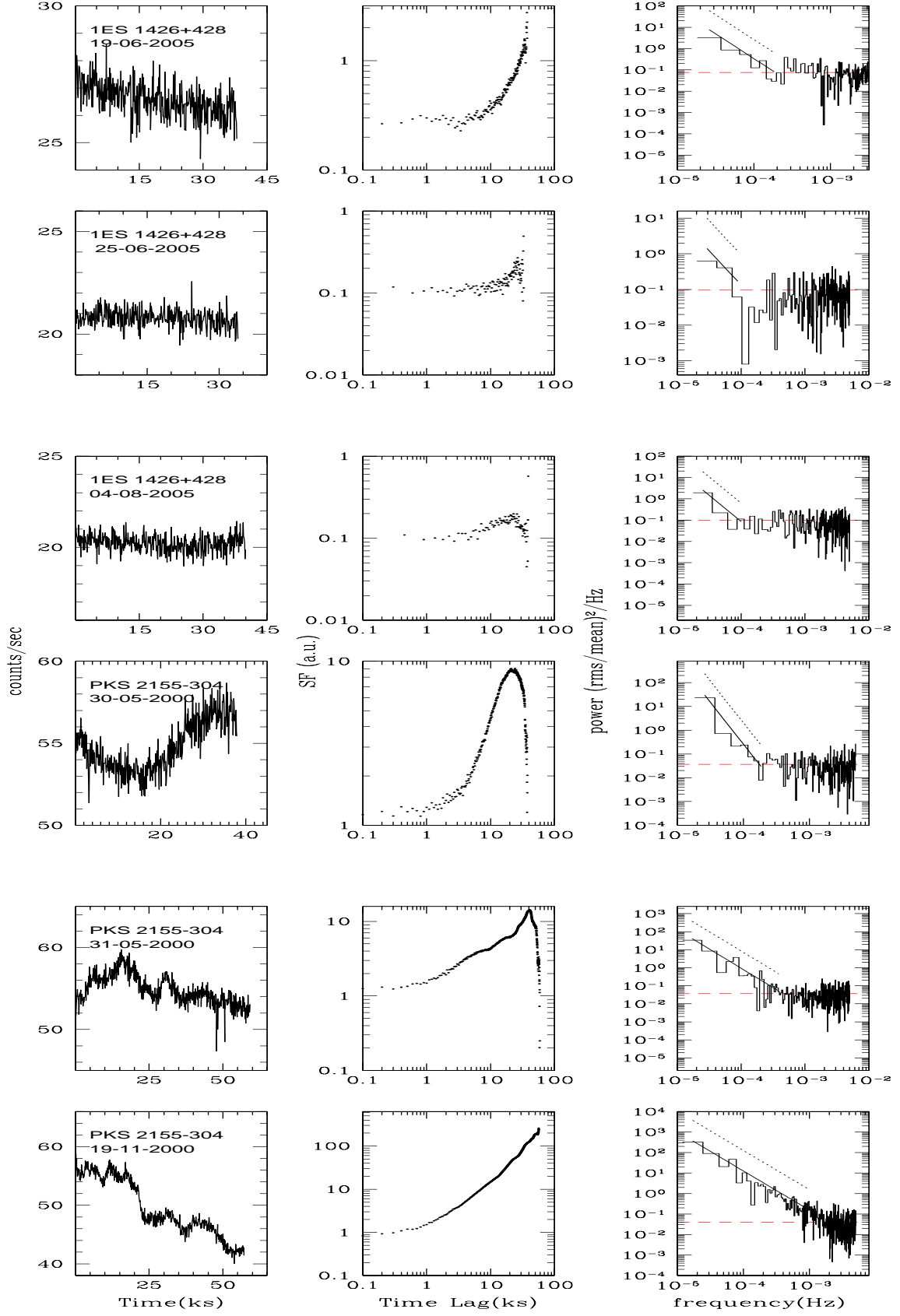


FIG. 2.— As in Fig. 1 for 1ES 1426+428 and PKS2155–304.

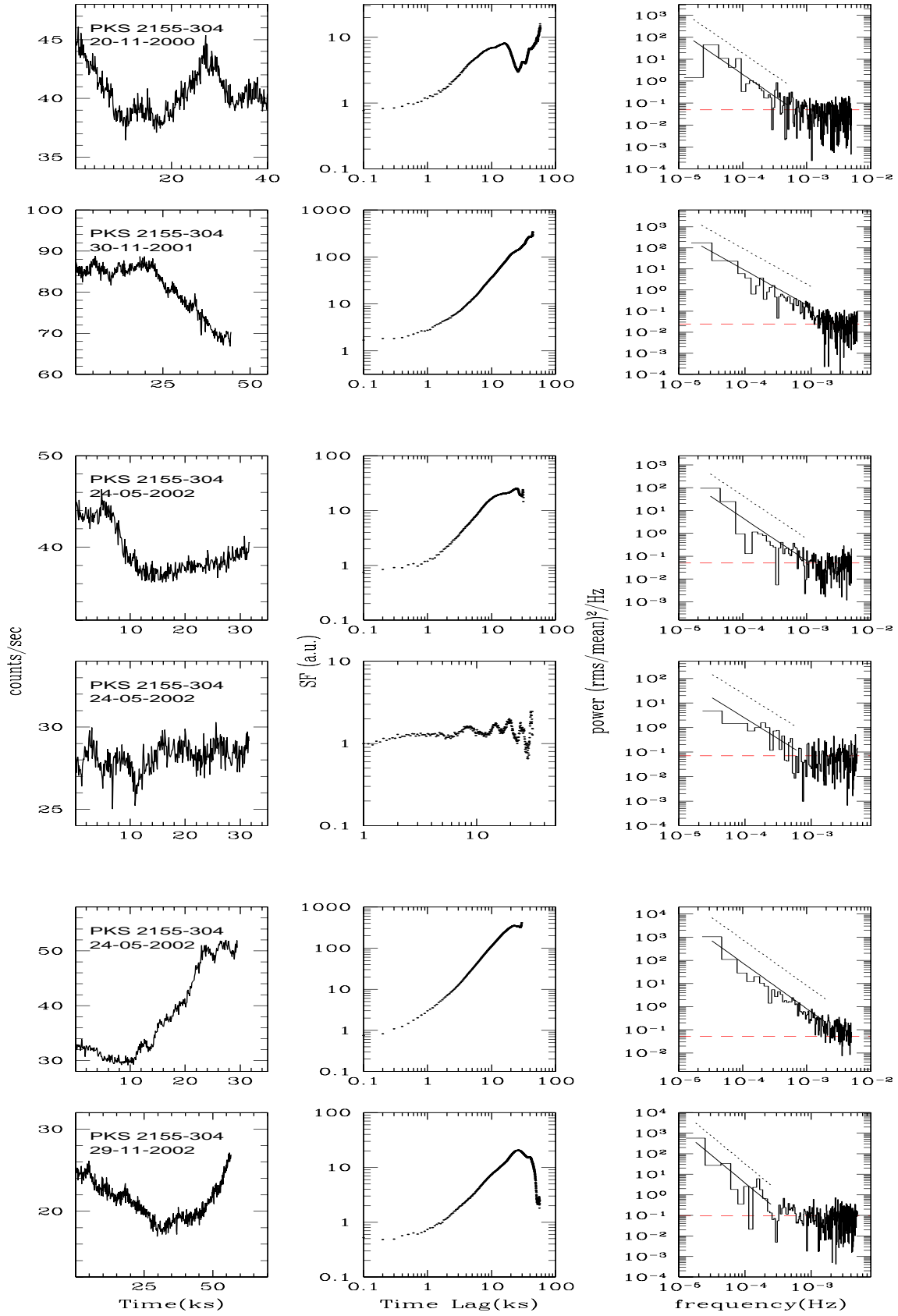


FIG. 3.— As in Fig. 1 for PKS2155–304.

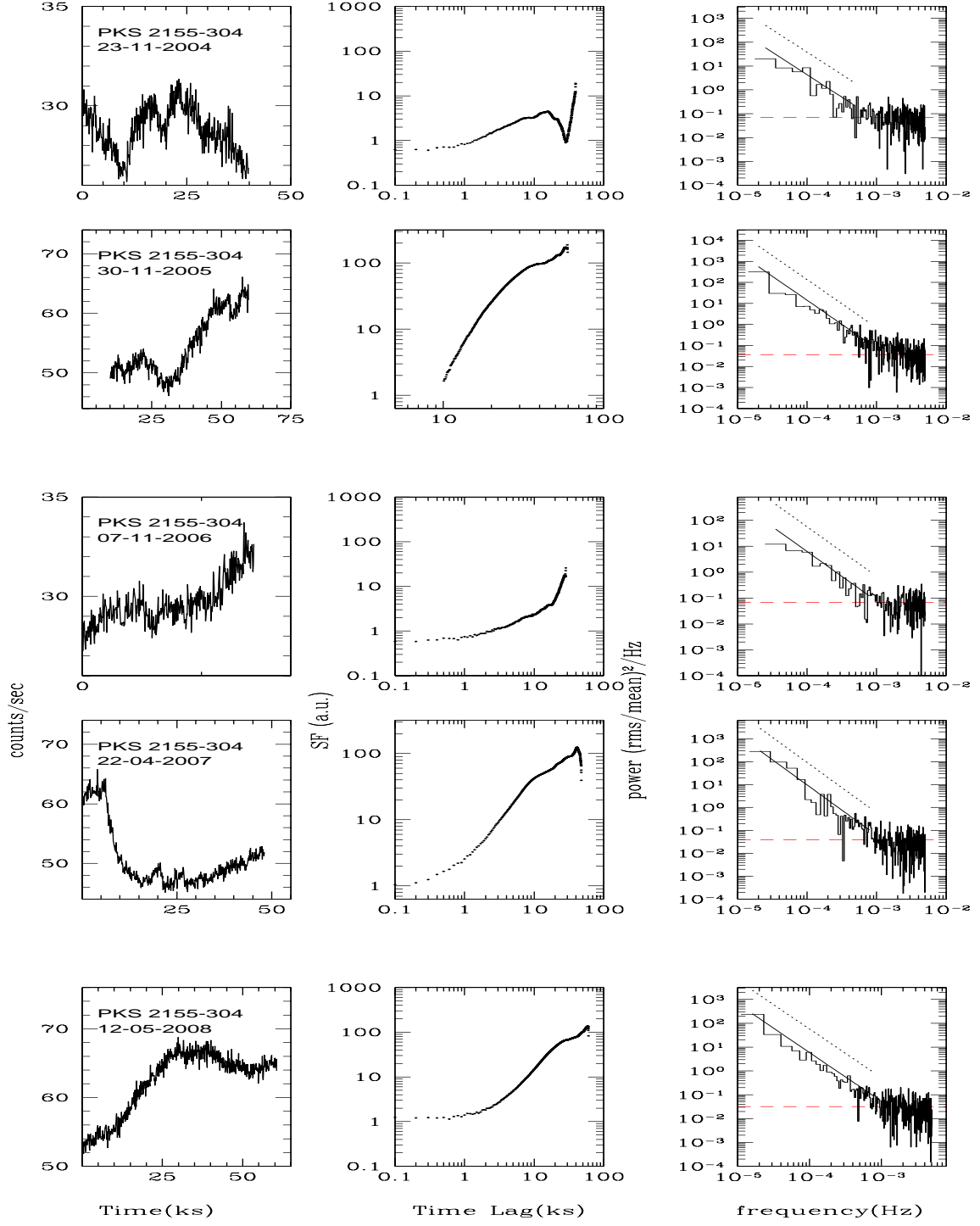


FIG. 4.— As in Fig. 1 for PKS2155–304.